Applied Energy 138 (2015) 496–504

Contents lists available at ScienceDirect

Applied Energy

journal homepage: www.elsevier.com/locate/apenergy

An inverse method for calculation of thermal inertia and heat gain in air conditioning and refrigeration systems

M.A. Fayazbakhsh *, F. Bagheri, M. Bahrami

Laboratory for Alternative Energy Conversion (LAEC), School of Mechatronic Systems Engineering, Simon Fraser University, 250-13450 102 Avenue, Surrey, BC V3T 0A3, Canada

HIGHLIGHTS

- An inverse method is proposed to calculate thermal inertia in HVAC-R systems.
- Real-time thermal loads are estimated using the proposed intelligent algorithm.
- Calculation algorithm is validated with on-site measurements.
- Freezer duty cycle data are extracted only based on temperature measurements.

ARTICLE INFO

Article history:
Received 9 February 2014
Received in revised form 25 October 2014
Accepted 1 November 2014
Available online 16 November 2014

Keywords:
HVAC-R
Thermal inertia
Heat gain
Inverse method

ABSTRACT

A new inverse method is proposed for estimation of thermal inertia and heat gain in air conditioning and refrigeration systems using on-site temperature measurements. The method is applied on a walk-in freezer room of a restaurant in Surrey, British Columbia, Canada during one week of its regular operation. The thermal inertia and instantaneous heat gain are calculated and the results are validated using actual information of the materials inside the freezer room. The proposed method can be implemented in intelligent control systems designed for new and existing HVAC-R systems to improve their overall energy efficiency and reduce their environmental impacts.

1. Introduction

Heating, Ventilation, Air Conditioning, and Refrigeration (HVAC-R) contribute to a tremendous portion of the global energy consumption in a wide array of residential, industrial, and commercial applications worldwide. HVAC-R consumes half of the energy use in buildings and 20% of the total national energy use in European and American countries [1]. Predictions indicate a further increase of 50% from the current figure during the next 15 years in the European Union countries [1]. Furthermore, Air Conditioning (AC) is the second most energy consuming unit in vehicles [2]. In an electric vehicle, AC power consumption can be as high as 12% of the total vehicle power during regular commuting [3]. As such, efficient design of new HVAC-R systems and devising intelligent control methods for existing systems can lead to significant reduction of total energy consumption and greenhouse gas emissions in large scales.

Proper design and intelligent operation of an HVAC-R system requires: (i) accurate prediction of thermal loads, and (ii) appropriate design and selection of the cooling unit. Accurate cooling load calculations are a prerequisite to proper sizing, selection, and control of any HVAC-R system. Modern air conditioning systems are equipped with feedback controllers that allow them to manipulate the operation of the HVAC unit in order to efficiently sustain thermal comfort. Although parameters such as room temperature, humidity, and occupancy level are used as control variables, it is advantageous to extend the first design step, *i.e.*, the load estimation to the operation stage of the unit. Real-time estimation and prediction of the upcoming thermal loads alongside raw measurements can be beneficial for energy-efficient control of HVAC systems, especially in Mobile Air Conditioning (MAC) applications that experience highly dynamic load variations.

In many applications, controllers based on on–off action or modulating control are successfully used that utilize the room temperature as the controlled variable [4]. Nevertheless, it is inherently impossible to predict upcoming thermal conditions by using conventional controllers that only rely on the current room status. It is shown that intelligent control of the HVAC operation based on

* Corresponding author. Tel.: +1 778 782 8538.
E-mail addresses: mfayazba@sfu.ca (M.A. Fayazbakhsh), mbahrami@sfu.ca (M. Bahrami).

http://dx.doi.org/10.1016/j.apenergy.2014.11.004
0306-2619/

prediction of the load can help maintain air quality while minimizing energy consumption [5,6]. By predicting thermal loads, controllers are enabled to not only provide thermal comfort in the current condition, but also adjust the system operation to cope with the upcoming conditions in an efficient manner. Thus, improvement of load calculation methods and the ability to estimate and predict the loads in real-time can improve the feedback information for the control of the HVAC system, which, in turn, result in significant reduction of total energy consumption and greenhouse gas emissions. Furthermore, in applications where the room contents may vary over time, an algorithm that can estimate the thermal inertia in an unsupervised manner can aid the HVAC-R system to adapt to the new conditions. Given the automatic adaptability of the HVAC-R system, it can be further controlled to perform at different capacities in order to reduce the overall energy consumption.

The American Society of Heating, Refrigerating, and Air Conditioning Engineers (ASHRAE) established an extensive methodology for calculation of heating and cooling loads. The heat balance method [7,8] is an example of such methods. It is a straight-forward and rigorous method that involves calculating a surface-by-surface heat balance of the surrounding walls of a room through consideration of all conductive, convective, and radiative heat transfer mechanisms. The method has been extensively used in residential and non-residential applications [5,6]. Mobile Air Conditioning (MAC), especially in electric vehicles, is also a crucial application where potential HVAC energy savings are possible. Less energy consumption by mobile HVAC systems directly results in higher mileage and better overall efficiency on the road [9]. Zheng et al. [10] devised a simple method to calculate thermal loads in vehicles. In their approach the different load categories such as radiation and ambient loads were considered. A case study was performed and the results were validated by experiments. Although their methodology has shown good agreement with experimental results, much details of the vehicle cabin and service conditions is needed to perform the necessary modelling calculations. Arici et al. [11] developed a computer code for simulation of the dynamic operation of a climate control system in a typical vehicle. Khayyam et al. [12] collected a set of models to calculate the different categories of thermal loads encountered in a vehicle. After using appropriate models for calculation of each of the load categories, they implemented control algorithms to improve the overall efficiency of the mobile air conditioning system.

In many applications, thermal loads vary dynamically. Novel approaches are being studied in the literature for real-time estimation of thermal loads. Several methodologies are introduced in the literature for estimation of thermal loads in existing buildings. Kashiwagi and Tobi [13] proposed a neural network algorithm for prediction of thermal loads. Ben-Nakhi and Mahmoud [14] also used general regression neural networks and concluded that a properly-designed neural network is a powerful tool for optimizing thermal energy storage in buildings based only on external temperature records. They claimed that their set of algorithms could learn over time and improve the prediction ability. Li et al. [15] presented four modeling techniques for hourly prediction of cooling loads. The methods included back propagation neural network (BPNN), radial basis function neural network (RBFNN), general regression neural network (GRNN), and support vector machine (SVM). Other researchers have used fuzzy control algorithms to propose load prediction methods. Among many, Sousa et al. [16] developed a fuzzy controller to be incorporated as a predictor in a nonlinear model-based predictive controller. Wang and Xu [17,18] used a Genetic Algorithm (GA) for identification of parameters in a model for estimation of thermal performance. In their approach, a thermal network of lumped thermal masses and parameters was identified using operation data and GA estimators.

A disadvantage of most existing load calculation methods is that they require much information about the air-conditioned space to estimate the loads. For instance, the heat balance method requires knowledge of material properties, thickness of walls, geographical location, fenestration data, weather information, occupancy, appliances, and other detailed information. Such an approach rarely relies on feedback information from the existing air-conditioned space. That type of methodology is a "forward" approach which makes the redesign/retrofit of existing HVAC-R systems a laborious and time-consuming task.

Alongside forward approaches, ASHRAE also recognizes data-driven or "inverse" methods of load calculation [7]. The data-driven modelling methodology consists of gathering the performance data of an existing system and analyzing them. Relatively few parameters are required in an inverse approach compared to forward methodologies. In an inverse method, model parameters may be deduced from the room data. Thus, the inverse model can predict the "as-built" system performance more accurately [7]. Inverse methods concentrate on the study of existing HVAC-R systems and allow the thermal performance of the system to be inferred based on measured temperature data. This is particularly convenient for retrofitting existing systems. Major input data to an inverse algorithm are the room temperature under regular operation, as well as the performance/capacity of the HVAC-R system. Therefore, in an inverse method, the entire system, *i.e.*, the conditioned space plus the HVAC-R unit is merely seen as a black box that is investigated for a period of time.

In this study, a new inverse methodology is proposed for identification of the duty cycles in a typical refrigeration system. The lumped thermal inertia and heat gains are quantitatively calculated. The present approach is scalable and is irrespective to the shape of the conditioned room. Therefore, it can be applied to any HVAC-R application. The proposed analysis enables an accurate and real-time calculation of thermal loads. Therefore, it can be used for intelligent control of the corresponding HVAC-R unit. Many existing HVAC-R devices are equipped with constant-speed compressors and fans. Nevertheless, Qureshi and Tassou [19] reviewed the application of variable-speed capacity control in refrigeration systems. They argued that in order to compensate for half-load usage conditions, the option of variable-speed compressor consumed the least percentage of the full load power compared to other methods. Hence, implementation of the present algorithm combined with variable-speed compressors can further reduce the energy consumption and environmental impact of HVAC-R systems.

In the following sections, the acquisition of experimental data is first explained. Based on the collected data of the sample refrigeration system, the proposed model is discussed in a subsequent section. Results of the modelling approach are finally presented and the accuracy of the results is validated using experimental information of the freezer room.

2. Experimental study

A freezer room in a restaurant in Surrey, British Columbia, Canada was selected to collect data during its regular operation. Fig. 1 shows a picture of the inside of the walk-in freezer room as well as a 3D schematic of it. Dimensions of the room are shown in Fig. 1 as well.

Temperature sensors were installed in different locations inside the freezer room. Temperature data loggers (Track-It, Monarch Instruments) were used for logging the room temperature over a period of one week. The maximum error of the temperature data loggers is ±1 °C for the range of −20 °C to 85 °C. Fig. 2 shows the 7 locations where temperature data loggers were installed.

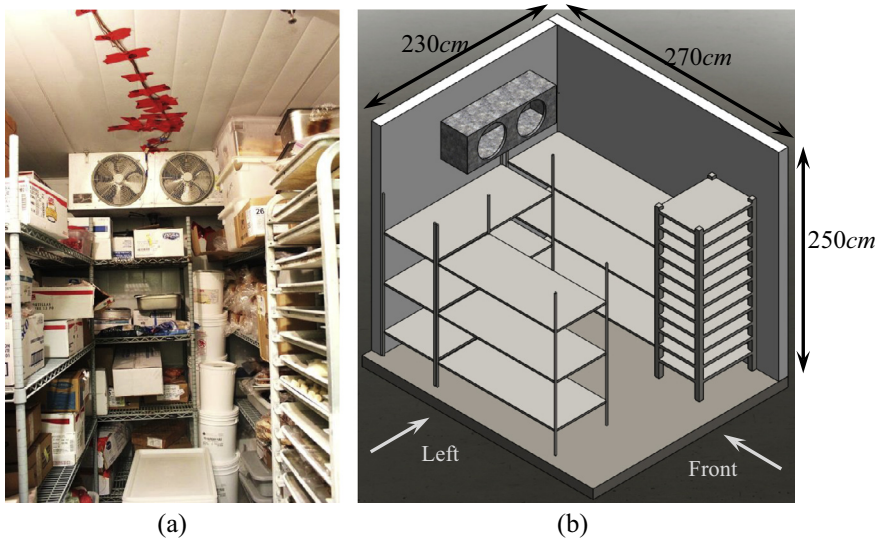

Fig. 1. (a) A picture of the freezer room. (b) 3D schematic of the freezer room with dimensions.

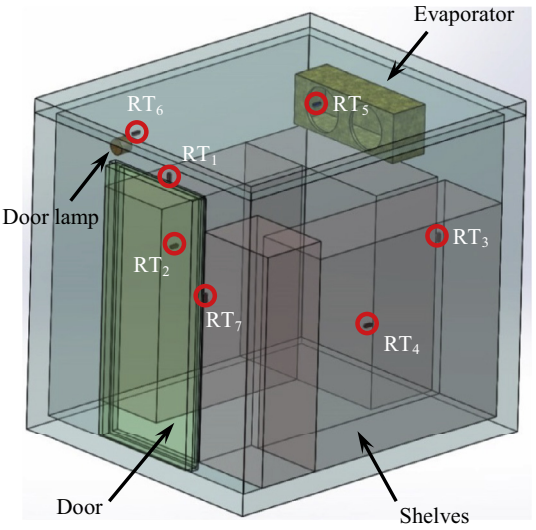

Fig. 2. Location of temperature data loggers in the freezer room. RT_1: above door, RT_2: left shelf, RT_3: back shelf, RT_4: right shelf, RT_5: ceiling, RT_6: beside door lamp, RT_7: beside door hinge.

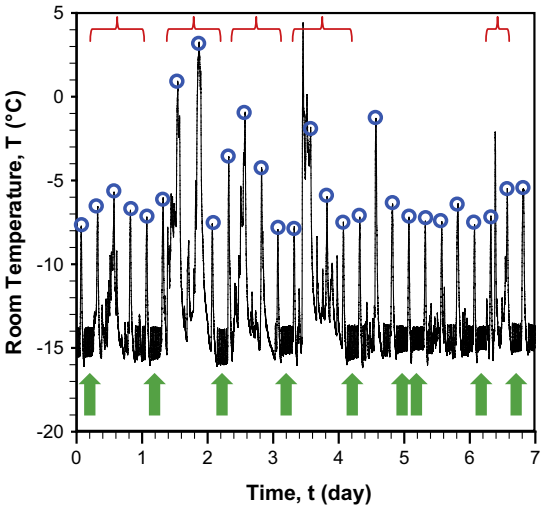

Fig. 3. Average temperature in the freezer room from 28 August 2013 at 00:01 am until 3 September 2013 at 11:59 pm. Arrows highlight noticeable temperature swings between low and high temperature set points, brackets show heavy duty periods, and circles denote temperature spikes due to defrosting.

Temperature was measured in various locations to determine its non-uniformity inside the room. It was observed that a temperature non-uniformity of less than 2 °C existed throughout the room. Therefore, an average value was used in the analysis to represent the lumped freezer room temperature.

Variations of the freezer room average temperature are shown in Fig. 3. The data show one week of freezer regular operation from 28 August 2013 at 00:01 am until 3 September 2013 at 11:59 pm. The freezer room was studied during 5 months from August 2013 to December 2013. Similar trends were observed throughout the period of study, since the freezer is placed in an air-conditioned indoor restaurant area and there is negligible direct influence from the outdoor temperature on the room performance. Therefore, the above-mentioned weeklong data is selected for the present analysis.

The freezer room in this study, as well as most existing refrigeration units, is controlled based on low and high temperature set points. Consequently, the system produces cooling until the room temperature reaches the low temperature set point. Once the minimum temperature is reached, the thermostat shuts the refrigeration unit down. At this point, the decrease of the room temperature stops and the temperature begins to increase as a result of heat gains. Consequently, the temperature increases until it reaches the high temperature set point. Once this maximum tolerable set point is reached, the thermostat triggers the refrigeration unit to switch back on. The low and high temperature set points are settings of the room thermostat and they can also be inferred from the temperature measurements, Fig. 3. By using the measured temperature at a location other than the thermostat, there can be a discrepancy between the actual thermostat set points and the apparent set points observed from the measurements. This is due to the temperature non-uniformity within the freezer because of which the set points may seem to vary on different days as well. To keep the generality of the approach for systems with the least available information, the apparent set points observed on the temperature data are used in this study.

Investigating the temperature graph shown in Fig. 3, the following 3 patterns are noticeable:

1. Swinging regimes

Temperature oscillations or swings occur mainly due to the starts/stops of the refrigeration unit. The period of these oscillations in the current application is approximately 20 min. Arrows show regions of swinging regime in Fig. 3. Fig. 4 shows a zoomed view of these oscillations. The apparent low and high temperature set points are identified from Fig. 4 to be −15.1 °C and −13.8 °C, respectively.

2. Temperature spikes

Rapid temperature increases are noticeable in some areas of Fig. 3. They are due to the occurrence of defrosting in the freezer. Defrosting is a process that melts the frost away from evaporator coils and is unavoidable for most systems. The defrost system can work either by heating the evaporator coils or turning off the system [20]. An automatic defrost system exists in the studied freezer room which kicks in every 6 h and heats up the evaporator coils to melt the frost. The defrost events, even though a necessity, impose a huge amount of heat load on the freezer room, as perceived by the sharp temperature increases in Fig. 3.

3. Heavy duty periods

Periods of heavy duty imposed on the refrigeration unit are also visible in certain times of specific days. In Fig. 3 they are denoted by irregular and random-looking variations in the freezer temperature. Since the temperature is mostly above the set points, it means that the condensing unit has been constantly on during these periods. Heavy duty periods depend on the usage pattern and are demarcated using brackets in Fig. 3. It is observed in Fig. 3 that the irregularities in temperature rise mostly occurred during daytimes of the first 4 days of measurements. In contrary, the next 3 days mostly showed swinging regimes and defrost spikes. It can be concluded from Fig. 3 that door openings and loading/unloading of goods in the freezer room considerably contribute to changes in the heat gain of the freezer room.

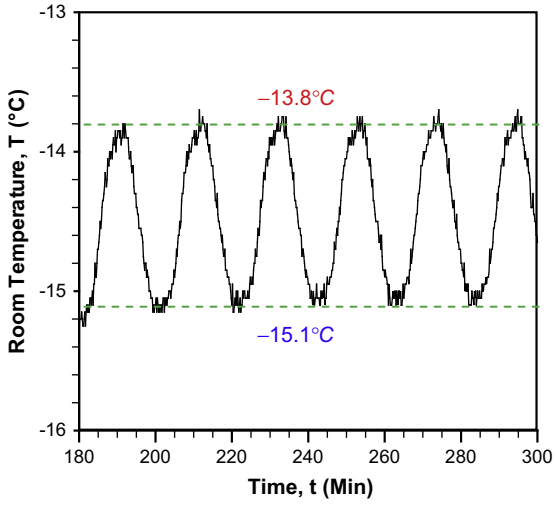

Fig. 4. Sample pattern of temperature swinging between low and high set points. The data shows the room temperature on 2 September 2013 from 03:00 am until 05:00 am. Apparent low and high temperature set points are identified as −15.1 °C and −13.8 °C, respectively.

3. Present model

A lumped thermal model of the room is used to develop the present inverse model. The cold room is assumed as a black box of which little information is available. In contrary to the forward approach, the objective is to determine the thermal characteristics of the freezer room based on available experimental data. A lumped or zero-dimensional thermal model can be described by two characteristics of the freezer enclosure: (i) total thermal inertia and (ii) total instantaneous heat gain. The contributing components to the room heat gain can be categorized into the following:

1. *Direct gain:* from electrical equipment, light bulbs, human metabolic loads, etc.
2. *Ambient gain:* from convective and conductive heat transfer across room walls.
3. *Ventilation gain:* from infiltration of air into the room.
4. *Solar gain:* from solar radiation into the room.

The summation of the above heat gains equals the overall heat gain of the freezer room. The total instantaneous cooling load is not necessarily equal to the total heat gain [7]. Nevertheless, the net thermal energy transferred to the room contributes to the temperature variation rate of the cooled enclosure. Therefore, the cooling load provided by the refrigeration system must satisfy the following heat balance equation:

$$\dot{Q}_{Cooling} + \dot{Q}_{Gain} = M\frac{dT}{dt} \tag{1}$$

where $\dot{Q}_{Gain}$ is the total heat gain, $\dot{Q}_{Cooling}$ is the instantaneous cooling load provided by the refrigeration unit, M is the overall thermal inertia of the freezer room, T is the average room temperature, and t is time. Adopting an explicit and forward method for calculating the thermal inertia M and overall heat gain $\dot{Q}_{Gain}$ is complicated and requires detailed information of the specific room and stored goods. On the other hand, an inverse method makes an estimation of these two parameters possible based on measurements of room temperature and an analysis of the system performance. Fig. 5 summarizes the steps for the proposed analysis approach from data collection to the estimation of instantaneous thermal inertia and total heat gain.

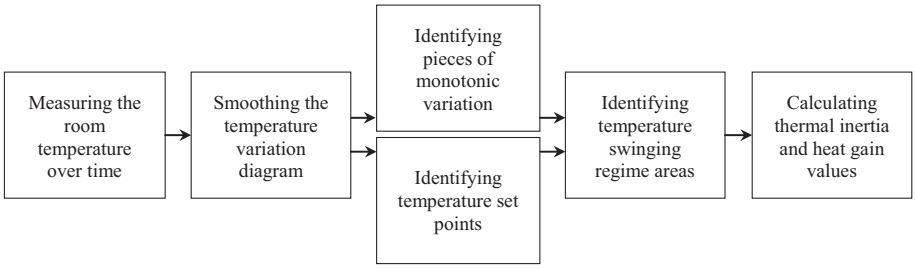

Fig. 5. Summarized algorithm of the proposed model.

In the first step, the room temperature is measured. Averaging and noises in temperature measurements can lead to a non-smooth temperature diagram. To ensure robust computations, it is important to first smooth the temperature fluctuations. Many noise reduction and smoothing algorithms are available in the literature. In this work, weighted averaging techniques similar to the one used in Smoothed Particle Hydrodynamics (SPH) [21] is used. The same technique is used to calculate the time derivative of the average temperature. The smoothing process may create inaccuracies, but is necessary for future steps where calculation of time derivatives is needed. Fig. 6 shows the smoothed temperature as well as its calculated time derivative for a sample piece of the data.

A numerical algorithm is developed that sweeps the data to find the time steps where the temperature derivative approaches zero. These time steps signify a change in the increasing or decreasing trend of the smoothed temperature. Once these extrema are found, the algorithm divides the temperature diagram into "pieces" which fall between them. Each piece is either monotonically increasing or decreasing. Fig. 7 shows a few of these data pieces identified by the algorithm. In order to present the piece-identification process more clearly, an exponential curve fit is provided for each of the pieces shown in Fig. 7. The specific period shown in Fig. 7 contains 16 pieces demonstrated by exponential correlations. These 16 pieces are numbered in Fig. 7. The pieces can be categorized into the following:

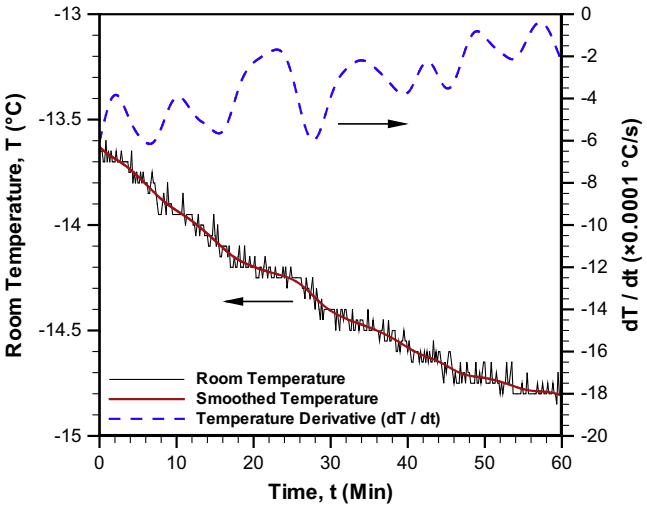

Fig. 6. Smoothing of the raw temperature and its calculated derivative with respect to time. The diagram covers the data for 1 September 2013 from 00:01 am until 01:00 am (see Fig. 3).

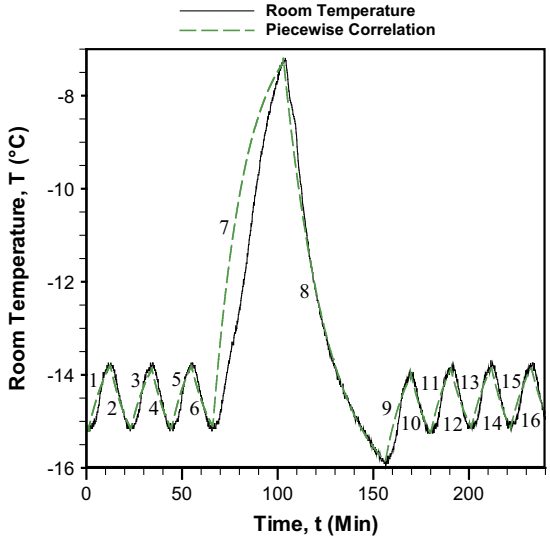

Fig. 7. Sample piece of temperature data for demonstration of pull-down and heat-gain processes. The data is divided into pieces as shown by piecewise exponential curve fits that are numbered in the figure. Temperature variations on 2 September 2013 from 00:01 am until 04:00 am are shown.

- Pull-down process

The data pieces where the temperature is decreasing are called pull-down processes. During pull-down processes, cooling effect is provided by the refrigeration unit to compensate the instantaneous heat gains and the thermal inertia of the freezer room. Therefore, the average room temperature is pulled down.

- Heat-gain process

The data pieces in which temperature is increasing are called heat-gain processes. Note that during heat gain, the refrigeration unit can be on or off depending on the room temperature status compared to the set points. During this process, the heat gain surpasses the potential cooling effect provided by the refrigeration unit, which in turn results in an increase in the average room temperature.

As previously discussed, the temperature diagram contains periods of freezer operation during which the temperature swings between the low and high set points. These oscillations are identified by consecutive pull-down and heat-gain processes. We also know that the temperature is below the high set point during any heat-gain process in the swinging regime. Therefore, the cooling system is turned off during such processes in the swinging periods. This is a key observation that allows the calculation of thermal inertia under such circumstances.

Assume a heat-gain process and its consecutive pull-down process within a temperature swinging period demonstrated in Fig. 4. The heat balance in Eq. (1) for the heat-gain process can be simplified to:

$$\dot{Q}_{Gain} = M\frac{\Delta T}{\Delta t}\bigg|_{Heat-gain} \tag{2}$$

since the refrigeration unit does not provide any cooling effect during the heat-gain period. Meanwhile, during the pull-down processes of the swinging regimes, cooling load is also provided to the freezer room. Therefore, the heat balance equation for any pull-down process takes the following form:

$$\dot{Q}_{Cooling} + \dot{Q}_{Gain} = M\frac{\Delta T}{\Delta t}\bigg|_{Pull-down} \tag{3}$$

where $\dot{Q}_{Cooling}$ has a negative value for cooling. Averaging over the time period of each piece, the time derivative dT/dt of Eq. (1) is replaced by $\Delta T/\Delta t$. Thus, a constant overall heat gain value can be calculated from Eqs. (2) and (3). $\Delta T = T_2 - T_1$ and $\Delta t = t_2 - t_1$ are the bulk changes in temperature and time during the process, respectively. Based on the definition, it is evident that $\Delta T/\Delta t > 0$ for heat-gain processes and $\Delta T/\Delta t < 0$ for pull-down processes.

Considering that the swinging regime occurs mostly at times when there is no change in the freezer room constituents (usually during nights when the door is shut and no goods are loaded or unloaded), we can assume that the thermal inertia of the system remains constant during the two processes of Eqs. (2) and (3). Since the door remains shut, the ventilation load is negligible during swinging regimes. The variation of temperature difference between the freezer room and the ambient air is also negligible,

since both the inside and outside temperatures are almost constant. This results in a relatively constant heat gain due to direct and ambient heat loads. Therefore, it can be reasonably assumed that the heat gain is constant between every two consecutive heat-gain and pull-down processes of a swinging period. Thus, knowing the cooling effect provided by the refrigeration unit, one can solve Eqs. (2) and (3) to arrive at the following relationship for the lumped thermal inertia of the freezer room:

$$M = \frac{\dot{Q}_{Cooling}}{\frac{\Delta T}{\Delta t}\Big|_{Pull-down} - \frac{\Delta T}{\Delta t}\Big|_{Heat-gain}} \quad (4)$$

Once the thermal inertia is known for a specific time, it is further used to find the average heat gain using Eq. (2) for heat-gain processes and Eq. (3) for pull-down processes.

4. Results and discussion

The analysis approach and the temperature data shown in Fig. 3 are implemented in a computer code for calculation of thermal inertia and heat gain. The algorithm detects periods of temperature swings. Once these periods are identified, the code calculates the room thermal inertia.

In order to use Eq. (4), it is necessary to know the cooling load $\dot{Q}_{Cooling}$ provided by the evaporator. In general, the provided cooling load varies by both the evaporator and condenser coil temperatures. Nevertheless, Eq. (4) is only applied during the mentioned swinging regimes when the evaporating temperature is oscillating in a narrow range between the set points. As a result, whenever the value of $\dot{Q}_{Cooling}$ is used in the present method, it merely represents the average cooling capacity of the system operating between the high and low set points. Jabardo et al. [22] and Wang et al. [23] showed that the cooling capacity varies by less than 5% due to 1 °C of evaporating temperature increase. Both studies show the same behavior for the dependence of the cooling capacity to the condensing temperature. Thus, although the cooling capacity is a function of the evaporating and condensing temperatures, its variation can be neglected for small changes in those temperatures.

Based on on-site measurements and the manufacturer information, the approximate cooling capacity provided by the studied refrigeration unit is $\dot{Q}_{Cooling} = -950$ W while the freezer temperature is swinging within the high and low set points. Since the condenser is placed in a restaurant indoor space, the condensing temperature is maintained relatively constant. Furthermore, since the set points are only 1.3 °C apart, as observed in Fig. 4, the evaporator also experiences a relatively constant temperature during the temperature swinging regimes. Thus, the freezer performance is negligibly affected by the variations of evaporator and condenser temperatures, and the provided cooling capacity can be assumed constant at $\dot{Q}_{Cooling} = -950$ W. The negative sign shows the direction of heat transfer from the room to the outside environment.

To verify the assumption of constant cooling load, further measurements are performed on the studied refrigeration cycle. Fig. 8 shows the air temperature at the inlet and outlet of the evaporator fan as measured by T-type thermocouples (5SRTC-TT-T-30–36, OMEGA®) during the same period of study (28 August 2013–3 September 2013). The thermocouples have an accuracy of ±1 °C and are installed at the inlet and outlet of the evaporator fan. Fig. 8 shows the measured evaporator temperatures for an arbitrary instance of the swings demonstrated in Fig. 4. When the cooling system is turned off, the inlet and outlet evaporator temperatures are almost equal and a heat-gain process occurs. During the cool-down processes, on the other hand, there is almost a constant gap between the temperatures which hints a relatively constant cooling load.

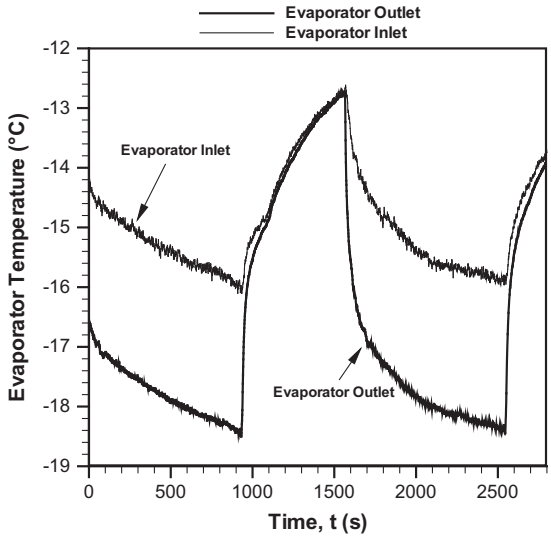

Fig. 8. Air temperatures at the inlet and outlet of the evaporator during an instance of temperature swing between the high and low set points.

The volumetric flow rate of the evaporator fan is measured to be 600 CFM which is equivalent to a mass flow rate of 0.38 kg in the corresponding temperature range shown in Fig. 8. The sensible cooling capacity is thus calculated as:

$$\dot{Q}_{Cooling} = \dot{m} c_p (T_o - T_i) \quad (5)$$

where $\dot{m}$ is the air mass flow rate, c_p is the air specific heat, T_o is the evaporator outlet air temperature, and T_i is the evaporator inlet air temperature. Fig. 9 shows the cooling capacity calculated based on the data shown in Fig. 8 and Eq. (5). As observed in Fig. 9, the cooling capacity is zero during the heat-gain processes. But during the pull-down processes, the cooling capacity oscillates around a constant value of almost $\dot{Q}_{Cooling} = -950$ W. The cooling capacity in Fig. 9 does not show a significant trend or variation during the swing regime. Accordingly, the excessive calculations and measurements required for the instantaneous cooling load can be avoided and a constant cooling capacity can be used in relevant applications of the proposed method without remarkable loss of accuracy. The same assumption is used in the rest of this study.

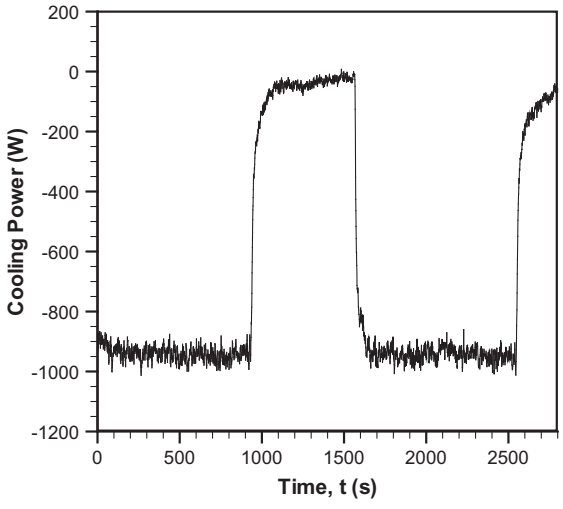

Fig. 9. Cooling power provided by the refrigeration system during an instance of temperature swing between the high and low set points.

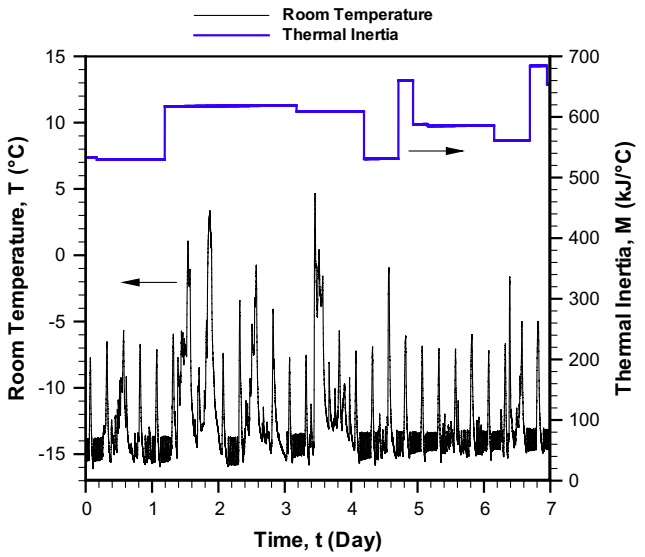

Fig. 10. Thermal inertia calculation results for the freezer room from 28 August 2013 at 00:01 am until 3 September 2013 at 11:59 pm.

Fig. 10 shows the calculation results for room thermal inertia during the period under consideration. Since the freezer is regularly used by the restaurant personnel for storing foodstuff, the contents of the room vary during the daytime. It can be inferred from the temperature variations of Fig. 10 that during daytime the freezer room experienced several events of door opening, which resulted in random temperature values far above the set points. Therefore, the swinging heat-gain and pull-down processes, occurring during night times, have been used to estimate the thermal inertia until the next occurrence of temperature swing pattern.

Fig. 11 shows the estimated heat gain values. The heat gains are calculated for every time step based on the thermal inertia information inferred from Fig. 10 and Eqs. (2) and (3). For the sake of clarity, only results covering the first 12 h of the refrigeration unit operation on 2 September 2013 are shown in Fig. 11. As mentioned in Fig. 3, there are 3 different temperature variation regimes: swinging regimes, temperature spikes, and heavy duty periods.

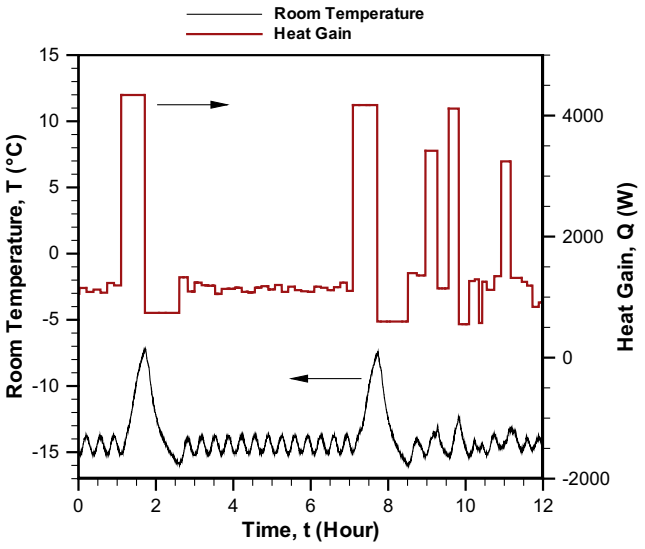

Fig. 11. Heat gain variations calculated on 2 September 2013 from 00:01 am until 12:01 pm. See Figs. 3 and 8 for temperature and thermal inertia information during the entire week of study.

The data shown in Fig. 11 are chosen so they contain the 3 different patterns in order to show the capability of the present method for handling all of them.

It is noticeable in Fig. 11 that the defrost events that occur at hours 1 and 7 impose significant amounts of load on the room. The instantaneous heat gain values jump to above 4 kW during defrost events which result in fast increase of temperature in the freezer room. As previously mentioned, the defrost events are set to automatically occur every 6 h with no monitoring and sensing of ice formation on the evaporator coils. Nevertheless, there is a considerable energy-saving potential in using intelligent defrost units [24].

According to Fig. 11, during the temperature swings of hour 1 as well as hours 3–7, the heat gain is estimated to be at almost the same level as the cooling power provided by the refrigeration cycle. As a result, the temperature is kept at a relatively constant level in a swinging manner. During the defrost spikes of hours 2 and 8, there are 2 distinct heat-gain and pull-down processes. In the heat-gain section of defrost events, there is a large 4 kW heat load imposed on the freezer from the heater-based defrost system. On the other hand, during the pull-down section of defrost events, there is less heat gain imposed on the freezer, since the defrost heater is off. Furthermore, notice that the heat gain is a direct function of the temperature difference between the freezer air and ambient air. At the peak of the defrost spike, there is a minimum difference between the inside and ambient air temperatures. As a result, the amount of heat gain in the pull-down section of a defrost event is even less than the steady heat gain of swinging regimes.

The heavy duty part of Fig. 11, covering hours 8–12, demonstrates random variations in the heat gain level. During this period of time, several cases occur when the restaurant personnel open the freezer door and allow large heat transfers from the ambient air into the freezer through a convective ventilation mechanism. Nevertheless, whenever the door is closed, the temperature is decreased and the amount of heat gain is also reduced to the levels governed by wall heat fluxes.

Table 1 lists the daily-averaged thermal inertia and heat gain values of the freezer room. The present inverse method allows the identification of the usage pattern in the freezer room based on temperature measurements. For instance, as listed in Table 1, some goods are added to the freezer room on 29 August 2013 resulting in an increase of the overall room thermal inertia by 70 kJ/°C compared to the previous day. Such information that are inferred from temperature measurements can help retrofit existing systems in real-time while knowing little else about the freezer. Daily-averaged heat gain values are also reported in Table 1. It is apparent that relatively higher lumped heat gains are encountered during 31 August 2013. Consistent with this observation is the fact that in Fig. 3, many more door opening occurrences were observed in the first 4 days of measurements.

A detailed list of foodstuff stored in the freezer room with their corresponding weight and thermal inertia is prepared based on

Table 1
Calculated daily-averaged thermal inertia and heat gain in the freezer room.

Date	Daily-averaged thermal inertia (kJ/°C)	Daily-averaged heat gain (W)
28 August 2013	519	1872
29 August 2013	589	2113
30 August 2013	606	2034
31 August 2013	599	2041
1 September 2013	566	1711
2 September 2013	573	1751
3 September 2013	588	1753
Average	577	1896

Table 2
Measured mass and thermal inertia values for the freezer contents on 31 August 2013.

Product	Mass (kg)	Thermal inertia (kJ/°C)
Chicken cages	25.00	43.00
Dry ribs	25.00	38.50
Sliced pepperoni	5.00	7.75
Sockeye	10.00	15.70
Shrimp	10.00	17.20
Halibut	25.00	41.75
Lobster	6.00	10.32
Calamari squid	25.00	42.00
Crab meat chunky	25.00	43.00
Albacore loin	5.00	8.80
Fries	15.00	21.15
Spicy chorizo	5.00	7.75
Sweet potato fries	7.50	11.93
Hash browns	15.00	21.15
Multi grain bread	2.10	3.47
White bread	3.80	6.27
Pesto	3.00	5.64
Corn	12.00	17.04
Peas	12.00	11.04
Raspberries	5.00	8.80
Red tortilla	0.02	0.04
Green tortilla	0.02	0.04
Whole wheat tortilla	0.02	0.04
Flour tortilla	25.00	41.25
Gluten free pizza shells	25.00	40.00
Gluten free buns	25.00	40.00
Brioche buns	25.00	42.50
Chocolate shaving	2.50	3.18
Vanilla ice cream	11.00	18.37
Miscellaneous parts	100.00[a]	60.00[a]
Total	455	628

[a] Estimated value.

on-site measurements. Existing tabulated values in ASHRAE Handbook of Fundamentals [7] are used for calculation of thermal inertia. The collected data is used to validate the proposed inverse modelling approach. Table 2 shows the list of foodstuff stored in the freezer room during 31 August 2013. The sum of all measured thermal inertia values is considered as the total thermal inertia of the freezer room. Due to the demand-based addition and withdrawal of foods, the freezer contents have slightly changed during the week of study, but they are kept in roughly constant amounts to ensure steady fulfilment of kitchen orders. Thus, although these are the values of one sample day, they are also deemed to represent an average of the freezer contents for the whole week.

Both the mass and the specific heat of the miscellaneous objects such as the evaporator, lights, shelves, and boxes are considerably smaller than those of the foodstuff. For instance, the specific heat of carbon steel, aluminum, and copper are 0.49 kJ/kg °C, 0.91 kJ/kg °C, and 0.39 kJ/kg °C, respectively, and these values are considerably smaller than the thermal inertia of white bread and corn which are 1.65 kJ/kg °C and 1.42 kJ/kg °C, respectively. As a result, the miscellaneous thermal inertia can be neglected in many applications without significant loss of accuracy. Nonetheless, an estimation of the miscellaneous thermal inertia is calculated and added to the measured thermal inertia of the foodstuff in order to improve the validation. Assuming a combined mass of 100 kg for the miscellaneous objects including the evaporator coils and shelf structures, and using an average specific heat of 0.6 kJ/kg °C for the metallic components, the total miscellaneous thermal inertia is calculated as 60 kJ/°C. This value is added to the total freezer thermal inertia in Table 2.

The total measured value of the room bulk thermal inertia is 628 kJ/°C, while the calculated average value of thermal inertia for the whole week of study is 577 kJ/°C. Hence, there is a discrepancy of 8% between the calculated and measured thermal inertia.

There is generally no direct method for measuring the heat gain in an air conditioning or refrigeration application. Typically, a heat balance of the room alongside appropriate correlations is used to estimate the amount of heat gain prior to the system design. The results of these thermal analyses are often estimations of the heat gain and provide an approximate value that has acceptable accuracy for the specific application at hand. Following the same approach, geometrical, material, and thermal properties of the freezer room are measured and summarized in Table 3. Convective heat transfer coefficients are estimated using correlations from ASHRAE [7] for turbulent natural convection on vertical and horizontal flat plates. The walls are equipped with old polyurethane insulation which is degraded due to several years of operation, hence providing a poor thermal resistance. The degradation mechanisms can cause the polyurethane thermal resistance to decrease to half of its original value [25]. Based on the methodology of the heat balance method [7], the heat transfer across the closed walls of the room is estimated. The overall heat gain of the room air is thus equal to the summation of these wall heat fluxes:

$$\dot{Q}_{Gain} = \sum_{Walls} \frac{A(T_{Amb} - T)}{1/h_o + b/k + 1/h_i} \tag{6}$$

where A is the wall surface area, T_{Amb} is the ambient temperature, T is the room average temperature, b is the wall thickness, k is the average wall thermal conductivity, and h_o and h_i are the outside and inside convection heat transfer coefficients, respectively.

As observed in Fig. 4, the high and low set points are −13.8 °C and −15.1 °C, respectively. In order to find an approximate temperature difference between the ambient and room temperature during the swinging regimes, we assume the room temperature to be at the average of the set points, *i.e.*, $T = -14.5$ °C. The restaurant temperature was measured at several locations near the freezer room and the average value of $T_{Amb} = 22.0$ °C was obtained. Using the properties collected in Table 3, Eq. (6) yields to a total ambient heat gain value of $\dot{Q}_{Gain} = 1002$ W. During the swinging regions of Fig. 11, the calculated heat gain varies approximately between 1050 W and 1250 W, with an average value of $\dot{Q}_{Gain} = 1150$ W. Thus, although the heat gain and room temperature vary with time, a comparison of the average calculated value with the heat gain acquired from the heat balance analysis of the freezer room shows an error of less than 15%.

A future step in using the calculated results such as shown in Figs. 8 and 9 can be to utilize them in a dynamic control algorithm that modifies the supplied cooling load by the refrigeration unit based on the real-time thermal inertia and heat gain information.

Table 3
Geometrical, material, and thermal properties of the freezer room.

Location	Left	Back	Right	Front	Roof	Floor
Surface area, A (m^2)	6.7	5.7	6.7	5.7	6.2	6.2
Outside convective coefficient, h_o (W/m^2 °C)	2.8	2.8	2.8	2.8	0.6	3.1
Inside convective coefficient, h_i (W/m^2 °C)	2.8	2.8	2.8	2.8	0.6	3.1
Insulation thickness, b (cm)	3	3	3	3	3	3
Wall thermal conductivity, k (W/m °C)	0.06	0.06	0.06	0.06	0.06	0.06

Since the algorithm provides a real-time estimation of the instantaneous heat gain, a refrigeration unit equipped with a variable-speed compressor can be intelligently controlled to provide the instantaneous required cooling load to the freezer room. Such control algorithms might be able to reduce the annual energy consumption of air conditioning and refrigeration systems.

5. Conclusions

A new inverse method was proposed to estimate the real-time thermal inertia and heat gain in air conditioning and refrigeration systems based on on-site temperature measurements. The collected temperature data were smoothed and fed to a mathematical algorithm that detects periods of temperature swing between the set points. The pace and pattern of temperature variations during the swing regimes were utilized to calculate the thermal inertia and overall heat gain in the freezer room. Little information on the geometry, material, and usage pattern of the system were used which made the proposed algorithm ideal for inverse analysis and retrofit of existing refrigeration and air conditioning systems.

The algorithm was validated using experimental data collected from a walk-in freezer room of a restaurant in Surrey, British Columbia, Canada during a week of its regular operation. It was shown that several duty patterns could be recognized only by analyzing the temperature data over time. The inverse approach enabled us to interpret detailed information on the usage pattern of the freezer and to calculate the thermal parameters of the system. The method can be implemented in control systems of refrigeration units to reduce the overall energy consumption of stationary and mobile HVAC-R units.

Acknowledgements

This work was supported by Automotive Partnership Canada (APC), grant APCPJ 401826-10. The authors would like to thank the kind support of the Central City Brew Pub, 13450 102nd avenue, Surrey, British Columbia, Canada.

References

[1] Pérez-Lombard L, Ortiz J, Pout C. A review on buildings energy consumption information. Energy Build. 2008;40(3):394–8.
[2] Farrington R, Cuddy M, Keyser M, Rugh J. Opportunities to reduce air-conditioning loads through lower cabin soak temperatures. In: Proceedings of the 16th electric vehicle symposium; 1999.
[3] Lambert MA, Jones BJ. Automotive adsorption air conditioner powered by exhaust heat. Part 1: Conceptual and embodiment design. Proc Inst Mech Eng D: J Automob Eng 2006;220(7):959–72.
[4] Haines R, Hittle D. Control systems for heating, ventilating, and air conditioning. 6th ed. Springer; 2006.
[5] Khayyam H, Nahavandi S, Hu E, Kouzani A, Chonka A, Abawajy J, et al. Intelligent energy management control of vehicle air conditioning via look-ahead system. Appl Therm Eng 2011;31(16):3147–60.
[6] Khayyam H. Adaptive intelligent control of vehicle air conditioning system. Appl Therm Eng 2013;51(1–2):1154–61.
[7] ASHRAE. Handbook of fundamentals. Atlanta: American Society of Heating, Refrigerating and Air-Conditioning; 2009.
[8] Barnaby CS, Spitler JD, Xiao D. The residential heat balance method for heating and cooling load calculations. ASHRAE Trans 2005;111(1).
[9] Fayazbakhsh MA, Bahrami M. Comprehensive modeling of vehicle air conditioning loads using heat balance method. SAE Trans 2013.
[10] Zheng Y, Mark B, Youmans H. A simple method to calculate vehicle heat load. SAE Inter 2011.
[11] Arici O, Yang S, Huang D, Oker E. Computer model for automobile climate control system simulation and application. Inter J Appl Thermodyn 1999;2(2):59–68.
[12] Khayyam H, Kouzani AZ, Hu EJ. Reducing energy consumption of vehicle air conditioning system by an energy management system. In: 2009 IEEE intelligent vehicles symposium, vol. i, no. 1; 2009. p. 752–7.
[13] Kashiwagi N, Tobi T. Heating and cooling load prediction using a neural network system. In: Proceedings of 1993 international conference on neural networks, vol. 1. IJCNN-93-Nagoya (Japan); 1993. p. 939–42.
[14] Ben-Nakhi AE, Mahmoud Ma. Cooling load prediction for buildings using general regression neural networks. Energy Convers Manage 2004;45(13–14):2127–41.
[15] Li Q, Meng Q, Cai J, Yoshino H, Mochida A. Predicting hourly cooling load in the building: a comparison of support vector machine and different artificial neural networks. Energy Convers Manage 2009;50(1):90–6.
[16] Sousa JM, Babuška R, Verbruggen HB. Fuzzy predictive control applied to an air-conditioning system. Contr Eng Pract 1997;5(10):1395–406.
[17] Wang S, Xu X. Simplified building model for transient thermal performance estimation using GA-based parameter identification. Int J Therm Sci 2006;45(4):419–32.
[18] Wang S, Xu X. Parameter estimation of internal thermal mass of building dynamic models using genetic algorithm. Energy Convers Manage 2006;47(13–14):1927–41.
[19] Qureshi T, Tassou S. Variable-speed capacity control in refrigeration systems. Appl Therm Eng 1996;16(2):103–13.
[20] Allard J, Heinzen R. Adaptive defrost. IEEE Trans Ind Appl 1988;24(1):39–42.
[21] Monaghan JJ. Smoothed particle hydrodynamics. Rep Prog Phys 2005;68(8):1703–59.
[22] Saiz Jabardo JM, Gonzales Mamani W, Ianella MR. Modeling and experimental evaluation of an automotive air conditioning system with a variable capacity compressor. Int J Refrig 2002;25(8):1157–72. http://dx.doi.org/10.1016/S0140-7007(02)00002-6.
[23] Wang S, Gu J, Dickson T, Dexter J, McGregor I. Vapor quality and performance of an automotive air conditioning system. Exp Thermal Fluid Sci 2005;30(1):59–66.
[24] Bansal P, Fothergill D, Fernandes R. Thermal analysis of the defrost cycle in a domestic freezer. Int J Refrig 2010;33(3):589–99.
[25] Bomberg M, Kumaran M. Use of field-applied polyurethane foams in buildings. Institute for Research in Construction, National Research Council of Canada; 1999. p. 1–6.